2 Aroylthioureas and their Rhenium and Technetium Complexes

2.1 Benzoylthioureas

The first benzoylthioureas, which were prepared in a simple one-pot synthesis from benzoyl chloride, NH_4SCN and amines (Scheme 2.1), were reported by Irwin B. Douglass, and F. B. Dains in 1934 [15]. From this general procedure, N,N-dialkyl-N'-benzoylthioureas (HR^1R^2btu) [16] or N-alkyl-N'-benzoylthioureas (H_2Rbtu) [17] could be obtained by the use of secondary amines or primary amines. The use of aryldicarbonyldichlorides such as *m*-phthaloyl dichloride [18] and 2,6-dipicolinoyl dichloride [19] instead of benzoyl chloride gives access to aroyl bis(thioureas).

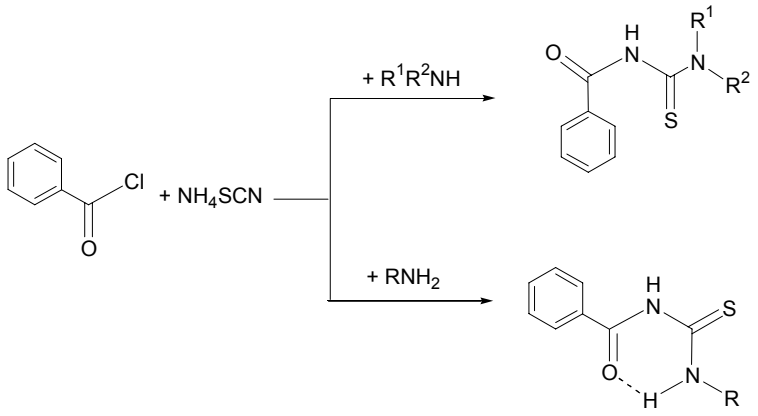

Scheme 2.1 Synthesis of HR^1R^2btu and H_2Rbtu.

In general, compounds of the type HR^1R^2btu are stable, relatively hydrophobic substances, with one dissociable proton on the weakly acidic amido C(O)NHC(S) moiety. For a series of hydrophilic N,N-dialkyl-N'-aroylthioureas, the acid dissociation constants, $pK_{a(NH)}$ have been found in the range from 7.5 to 10.9 in water–dioxane mixtures [20]. No similar information is available for the corresponding ligands H_2Rbtu with two dissociable protons, although there exists at least one metal complex in which the ligand H_2Rbtu coordinates as a doubly deprotonated anion [21].

2.1.1 Synthesis of N,N-Dialkyl-N'-benzoylthioureas and Aroylbis(N,N-dialkylthioureas)

The synthesis and spectroscopic characterization of N,N-dialkyl-N'-benzoylthioureas and aroylbis(N,N-dialkylthioureas) used in this work have been previously published [16,18,19]. The abbreviation scheme which is used throughout this work is presented in Chart 2.1.

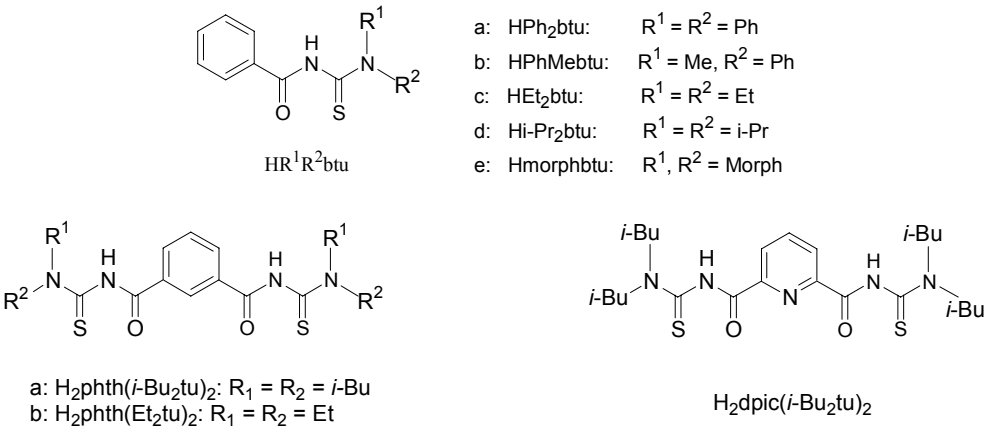

Chart 2.1 N,N-Dialkylbenzoylthioureas and aroylbis(N,N-dialkylthioureas) used throughout this work.

2.1.2 Synthesis of N-Picolyl-N'-benzoylthiourea (H_2picbtu)

Adopted from the general synthesis of benzoylthioureas, H_2picbtu can be prepared by subsequent reactions of benzoylchloride with ammonium thiocyanate and picolylamine. The product precipitates in high yields directly from the reaction mixture as a colourless, analytically pure, microcrystalline solid.

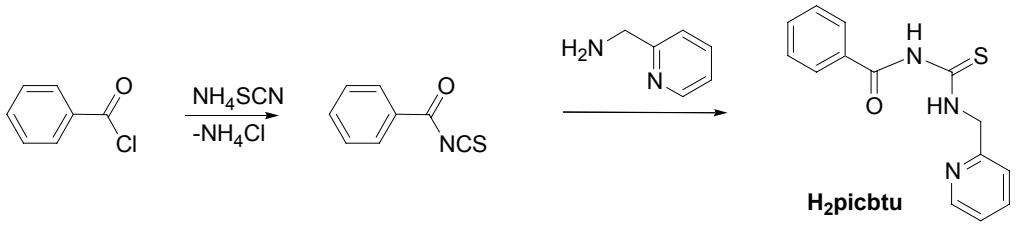

Scheme 2.2 Synthesis of H_2picbtu.

The IR spectrum of H_2picbtu is characterized by a strong broad absorption at 3186 cm^{-1} and a very strong absorption at 1666 cm^{-1} which can be assigned to the NH and C=O stretches. In the ^{1}H-NMR spectrum, the signals of the NH protons appear as one singlet and one triplet at 11.48 and 11.67 (J= 4.8 Hz) ppm, respectively. The C=O (180.28 ppm) and C=S (168.08 ppm) signals in the ^{13}C-NMR spectra are in the same region as those of other monoalkylthioureas [17c].

Single crystals of H_2picbtu suitable for an X-ray study were obtained by slow evaporation of a THF/iso-propanol solution. Figure 2.1 illustrates the structure of the ligand together with the intramolecular hydrogen bond between N6 and O5. This bond is sufficiently strong to stabilize the *Z* conformation of C2-N6 bond of the compound in the solid state. An additional intermolecular hydrogen bond is established between N3 and the sulfur atom of the

neighboring molecule. Selected bond lengths and angles are summarized in Table 2.1. The molecule is almost planar except of the phenyl ring which possesses a slight deviation from the mean plane formed by the rest of the molecule. While the C4-O5 and C2-S1 bonds of 1.222(2) Å and 1.676(1) Å are within the expected range of C=O and C=S double bonds, the C2-N3, N3-C4 and C4-N6 distances reflect partial double bond character. This structural feature has previously been found in other monoalkylbenzoylthiourea ligands and suggests that the protons are mainly located at the N3 and N6 atoms [17].

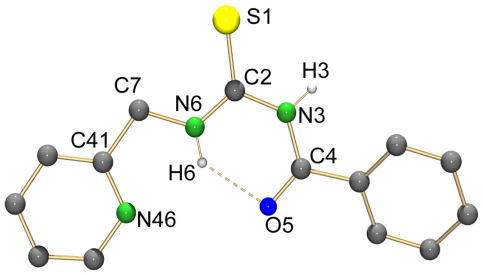

Figure 2.1 Molecular structure of H_2picbtu. Hydrogen atoms bonded to carbons were omitted for clarity.

Table 2.1 Selected bond lengths and angles in H_2picbtu

Bond lengths (Å)					
S1–C	1.676(1)	N3–C4	1.376(2)	C2–N6	1.315(2)
C2–N3	1.392(2)	C4–O5	1.222(2)	N6-C7	1.447(2)
Angles (°)					
S1–C2–N3	119.1(1)	C2–N3–C4	127.2(1)	C2–N6–C7	123.2(1)
S1–C2–N6	123.6(1)	N3–C4–O5	122.1(1)	N6–C2–N3	117.4(1)

Hydrogen bonds				
D-H…A	d(D-H)	d(H…A)	d(D…A)	<(DHA)
N(6)-H(6)...O(5)	0.86	1.96	2.6400(16)	134.6
N(3)-H(3)...S(1)#1[i]	0.86	2.58	3.4088(12)	162.8

(i) Symmetry transformations used to generate equivalent atoms: #1 -x,-y,-z

2.2 Rhenium and Technetium Complexes with Dialkylbenzoylthioureas

Despite HR^1R^2btu are quite old ligand systems, their coordination chemistry and potential applications have only been explored in the last three decades, pioneered by the work of Hoyer and Beyer [22]. These and other authors have published the coordination chemistry of HR^1R^2btu with a large number of transition metals [16]. In the majority of their structurally characterized complexes, they act as bidentate O,S-monoanionic ligands [23]. Coordination as

neutral, monodentate S-ligands are found in Ag(I) and Au(I) compounds and in a Pt(II) complex, [24] while examples of transition metal complexes with benzoylthioureas as bridging ligands are very rare [25,26]. The structural chemistry of square-planar bis-chelates of benzoylthioureas with d^8 or d^9 ions such as Ni(II), Pd(II), Pt(II) or Cu(II) is dominated by *cis* isomers [23c,27], and only a few crystal structures of *trans*-isomers have been elucidated [28]. Photochemical *cis/trans* isomerisation has been studied recently on Pt(II) and Pd(II) complexes, showing that the *trans* isomers are thermodynamically instable and readily re-form the *cis* compounds [29]. Exclusively facial coordination is observed for tris-chelates of HR^1R^2btu with Ru(III), Rh(III) and Co(III) [30].

Surprisingly less is known about rhenium and technetium complexes with benzoylthiourea-type ligands. There are only two structurally well characterized rhenium compounds: the neutral oxorhenium(V) complex $[ReOCl(Et_2btu)_2]$ (**1c**) and the tricarbonylrhenium(I) compound $[Re(CO)_3Br(HEt_2btu)_2]$ (**I**) [12,13] (Figure 2.2). The latter one is the only example where chelate formation is observed with a neutral HR_2btu ligand. Only one early report describes an synthetic approach to benzoylthioureato complexes of technetium by the reduction of pertechnetate in the presence of the ligands, and the formation of neutral $[Tc(R_2btu)_3]$ complexes was suggested on the basis of spectroscopic data [31]. This lack of knowledge is particularly surprising in the light that numerous thiourea complexes of rhenium and technetium have been studied extensively and found use as precursors for the synthesis of low-valent Re and Tc complexes [32].

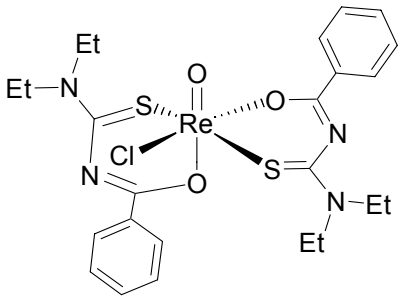

1c

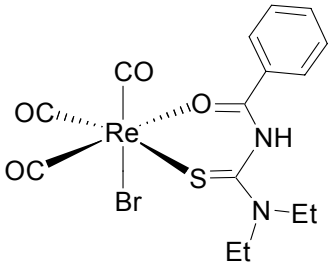

I

Figure 2.2 Previously reported benzoylthiourea complexes of rhenium. $[ReOCl(Et_2btu)_2]$ (**1c**) and $[Re(CO)_3Br(HEt_2btu)_2]$ (**I**).

2.2.1 Re^VO and Tc^VO Complexes with Dialkylbenzoylthioureas

Reactions between N,N-dialkylbenzoylthiourea ligands, HR^1R^2btu, and the common rhenium(V) starting material $[ReOCl_3(PPh_3)_2]$ proceed in different ways depending on the

used solvents and the reaction conditions applied. In absence of a supporting base, $[ReOCl_3(PPh_3)_2]$ does not react with HR^1R^2btu in polar solvents such as MeOH, EtOH or acetone even under reflux. This result is in accordance with the findings of Dilworth et al., [12] who were not able to isolate crystalline rhenium complexes with HEt_2btu when they started form this precursor. In CH_2Cl_2 solutions of dialkylbenzoylthioureas, however, the sparingly soluble $[ReOCl_3(PPh_3)_2]$ readily dissolves and yellow-green solutions are formed, which contain mixtures of $[ReOCl_2(PPh_3)(R^1R^2btu)]$ complexes as main products (**1**) and $[ReCl_2(PPh_3)_2(R^1R^2btu)]$ compounds as minor side-products (**6**) (Scheme 2.3).

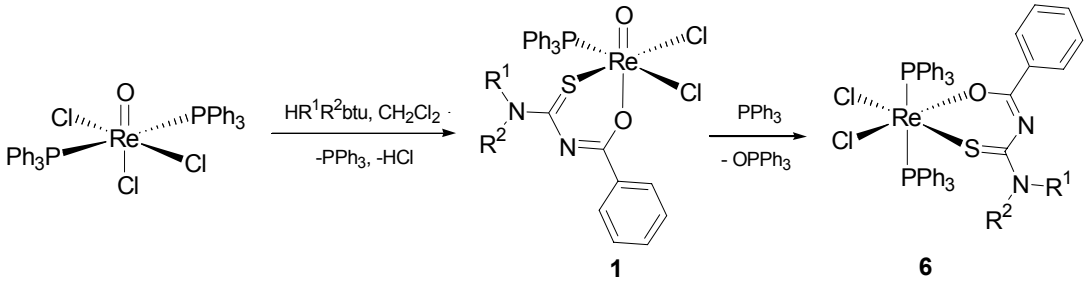

Scheme 2.3 Reaction of HR^1R^2btu with $[ReOCl_3(PPh_3)_2]$.

Infrared spectra of complexes **1** exhibit strong bands between 1400 and 1500 cm^{-1}, but no absorptions in the range between 1650 and 1690 cm^{-1}, where the $\nu_{C=O}$ stretches typically appear in the spectra of the non-coordinated benzoylthioureas. This corresponds to a bathochromic shift of more than 200 cm^{-1} and indicates chelate formation with a large degree of electron delocalization within the chelate rings as has been observed for other $R^1R^2btu^-$ chelates [16]. The absence of bands in the region of 3100 cm^{-1} indicates the expected deprotonation of the ligands during complex formation. Intense bands between 900 and 1000 cm^{-1}, which can be assigned to the Re=O vibrations [33], confirm the presence of oxo ligands in **1**.

FAB^+ mass spectra of complexes of type **1** show only less intense signals of the molecular ions. They strongly tend to combine with the matrix 4-nitrobenzylalcohol and, thus, ions of the composition $[M + NBA - 2Cl]^+$ represent peaks of high intensity for this type of complexes.

NMR spectra of complexes **1** provide additional evidence for the proposed composition and molecular structure of the complexes. The spectra are characterized by complex coupling patterns due to hindered rotation around the $C–NR^1R^2$ bonds. This has previously been described for the uncoordinated N,N-dialkylbenzoylthioureas and some metal complexes [27,34]. A rotational barrier of ΔG = -15.5 kcal/mole was determinded for HEt_2btu [34c], and an increase of this parameter was detected as a consequence of complex formation with

Ni(II), Pd(II) or Co(II) ions [34d]. Usually, two sets of signals are observed in ^{1}H and ^{13}C spectra of the Re complexes under study. This may lead to complex coupling patterns in the proton spectra as in that of **1e**, where the CH_2 protons show a complex array of overlapping multiplets in the range between 3.9 and 4.9 ppm and only the ^{13}C NMR spectra clearly show four separated resonances of these CH_2 groups at 49.68, 51.41 (CH_2N) and 67.00, 67.48 ppm (CH_2O).

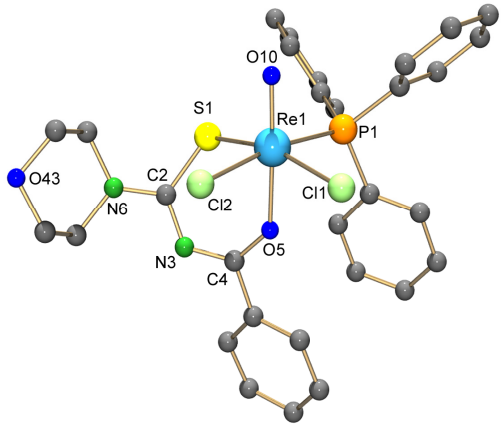

Figure 2.3 Molecular structure of [$ReOCl_2(PPh_3)$(Morphbtu)] (**1e**). Hydrogen atoms were omitted for clarity.

Table 2.2 Selected bond lengths (Å) in [$ReOCl_2(PPh_3)$(i-Pr_2btu)] (**1d**) and [$ReOCl_2(PPh_3)$(Morphbtu)] (**1e**)

	1d	**1e**		**1d**	**1e**
Re1–O10	1.679(4)	1.689(2)	Re1–Cl1	2.382(1)	2.379(1)
Re1–Cl2	2.405(1)	2.402(1)	Re1–S1	2.392(1)	2.400(1)
Re1–O5	2.068(3)	2.069(2)	Re1–P1	2.471(1)	2.464(1)
S1–C2	1.763(6)	1.761(3)	C2–N6	1.325(7)	1.323(4)
C2–N3	1.351(6)	1.342(4)	C4–O5	1.288(6)	1.289(4)
N3–C4	1.313(7)	1.315(4)			

Figure 2.3 depicts the molecular structure of compound **1e** as a representative for this type of complexes. Selected bond lengths compared to those in the analogous **1d** are listed in Table 2.2. The rhenium atoms exhibit distorted octahedral coordination geometry. Axial positions are occupied by an oxo ligand and an oxygen atom of the chelating ligand. The two chloro ligands of the equatorial coordination sphere are in *cis* arrangement to each other, and the rhenium atoms are located about 0.221 Å above the mean least-square plane, which is formed from S1, Cl1, Cl2 and P, towards the oxo ligand. The Re=O distances of 1.679(4)Å and 1.689(2) Å are in the expected range of rhenium–oxygen double bonds. A remarkable structural feature is the coordination of the benzoylic oxygen atom *trans* to the oxo ligand.

The Re–O5 bonds are expectedly longer than Re–O10, but reflect some double bond character as has been observed previously for a number of rhenium(V) complexes with oxo and alkoxo ligands in *trans* position [35]. Markedly longer Re-OR bonds are found when the alkoxo units are *cis* to the oxo unit [36]. Despite the fact that the chelate rings are not planar, a considerable extend of π-electron density is indicated by the observed bond lengths. The values of the C–S and C–O bonds are between those expected for carbon–sulphur and carbon–oxygen single and double bonds, and all C–N bonds including the C2–N6 bond are almost equal.

When acetone is used as solvent and NEt_3 is added as a supporting base, reactions of $[ReOCl_3(PPh_3)_2]$ and an excess of HR^1R^2btu ligands yield a second ligand exchange product and reduction to Re(III) compounds can be suppressed to a large extent. The different course of the reaction is indicated by a change of the colour of the reaction mixture from pale yellow-green to deep green. Green solids can be isolated upon concentration of such solutions, which consist of the bis-chelates $[ReOCl(R^1R^2btu)_2]$ (**2**), PPh_3, some traces of **1** and small amounts of dark unidentified side-products. Purification can be done either by several recrystallizations from acetone or by column chromatography using silica gel. The yields of such reactions can be improved by using a 5-fold excess of the ligands and a prolonged reaction time. A more facile approach to complexes of type **2** is the use of $(NBu_4)[ReOCl_4]$ as precursor (Scheme 2.4). Such reactions in methanol give **2** in excellent yields.

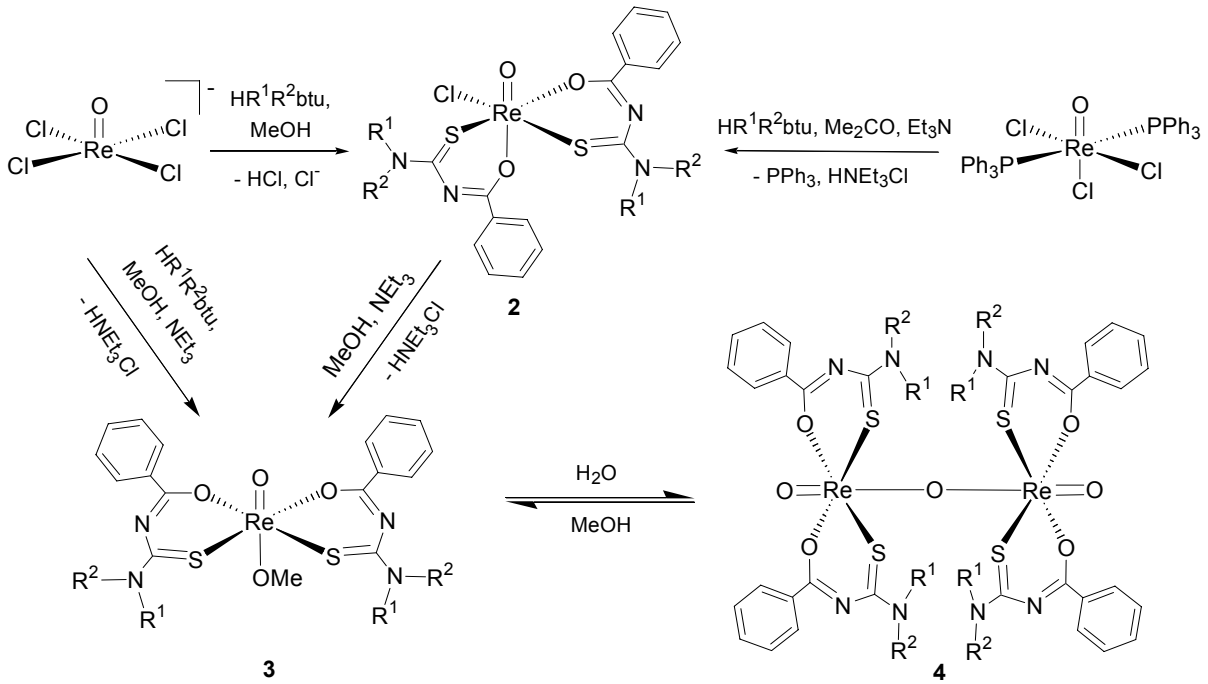

Scheme 2.4 Synthesis of $[ReOCl(R^1R^2btu)_2]$ (**2**), $[ReO(OMe)(R^1R^2btu)_2]$ (**3**), $[\{ReO(R^1R^2btu)_2\}O]$ (**4**) and reversible transformation between **3** and **4**.

IR spectra of **2** show intense bands between 950 and 990 cm^{-1} which can be assigned to Re=O vibrations. As discussed for complexes of type **1**, chelate coordination of the $R^1R^2btu^-$ ligands results in a strong bathochromic shift of the C=O bands, which appear in the spectra in the range between 1400 and 1500 cm^{-1} and strongly overlap with C=C and C=N bands.

Each two sets of resonances of the C=O and C=S carbon atoms in the ^{13}C NMR spectra of **2** indicate that the two organic ligands are magnetically inequivalent. The proton NMR spectra are complex due to hindered rotation. In the spectrum of **2b**, which contains the asymmetric PhMebtu$^-$ ligands, seven out of eight CH_3 signals, which can be expected due the possible Z,E isomerism of the ligands in such complexes, are resolved. Two of them, at 3.87 ppm and 3.96 ppm, dominate with a relative intensity of approximately 75 percent and might be assigned to the E,E isomer, which is also established in the solid state structure of the compound (Figure 2.4). The missing eighth signal of minor intensity is most probably overlapped by one of the others. Interestingly, the spectrum of the analogous technetium compound **3b** (*vide infra*) exhibits only one broad methyl signal indicating that the rotation barrier of the C–NPhMe bond is lower in the technetium compound.

The molecular structure of **2b** (Figure 2.4) confirms the results of the spectroscopic studies showing the rhenium atom in a distorted octahedral coordination environment with inequivalent PhMebtu$^-$ ligands. One of them binds with its oxygen atom *trans* to the oxo ligand, similar to the situation in **1**, while the second chelating ligands occupies two equatorial coordination positions. This has significant effects on the established chelate rings. That of the equatorial ligand is almost planar with maximum deviation from the mean least-square plane of the chelate ring of about 0.205 Å for atom Cl2, while the sulphur atom of the axial chelate ring is positioned out of a mean least-square plane formed by the atoms Re1, O5, C4, N3 and C2 by 0.367 Å. Selected bond lengths are summarized in Table 2.3. The bonding situation inside the chelate rings is best described with an extended π-system. The C–N bonds of the ring systems are very similar and it is evident that considerable π-electron density is transferred to the exocyclic C2–N6 and C12–N16 bonds. This explains the detection of isomers in the ^1H NMR spectrum of the compound.

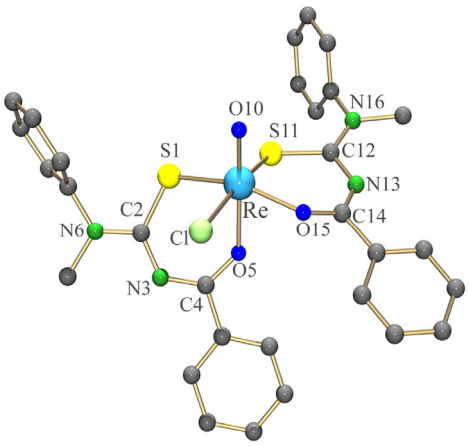

Figure 2.4 Molecular structure of [ReOCl(PhMebtu)$_2$] (**2b**). Hydrogen atoms were omitted for clarity.

Table 2.3 Selected bond lengths in [ReOCl(PhMebtu)$_2$] (**2b**)

Bond lengths (Å)			
Re1–O10	1.669(6) / 1.657(6)	Re1–Cl1	2.432(2) / 2.421(2)
Re1–S1	2.343(2) / 2.345(2)	Re1–S11	2.319(2) / 2.341(2)
Re1–O5	2.098(5) / 2.138(5)	Re1–O15	2.052(5) / 2.052(5)
S1–C2	1.760(8) / 1.752(8)	S11–C12	1.765(7) / 1.748(8)
C2–N6	1.33(1) / 1.35(1)	C12–N16	1.31(1) / 1.33(1)
C2–N3	1.33(1) / 1.33(1)	C12–N13	1.36(1) / 1.33(1)
N3–C4	1.33(1) / 1.32(1)	N13–C14	1.31(1) / 1.29(1)
C4–O5	1.287(9) / 1.280(9)	C14–O15	1.28(1) / 1.285(9)

* Two crystallographically independent species

Addition of a base such as NEt_3 to a refluxing solution of **2c** in MeOH causes an immediate color change from green to red and a complex of the composition [ReO(OMe)(Et_2btu)$_2$] (**3c**) is formed (Scheme 2.4). Structural analysis of the resulting purple solid reveals that besides the exchange of the chloro by a methoxy ligand, a rearrangement of the chelating ligands is generated. They are both found in equatorial positions in the product with the sulphur atoms *cis* to each other, while MeO^- is found *trans* to the oxo ligand. Both chelate rings are almost planar in **3c**, the molecular structure of which is shown in Figure 2.5. The obvious ability of ReO^{3+} cores to transfer electron density to alkoxo ligands in *trans* position and the higher degree of delocalized electron density in the equatorial chelate rings seem to be the driving forces of this ligand rearrangement. Several examples of rhenium(V) oxo/alkoxo complexes have been studied structurally before [35], and in all of these complexes the Re–OR bond is shorter than expected for a Re–O single bond. This is remarkable with respect to the oxo ligands in *trans* position, which should exert a

considerable *trans* influence and, thus, weaken these bonds instead of strengthen them. Selected bond lengths of **3c** are listed in Table 2.4.

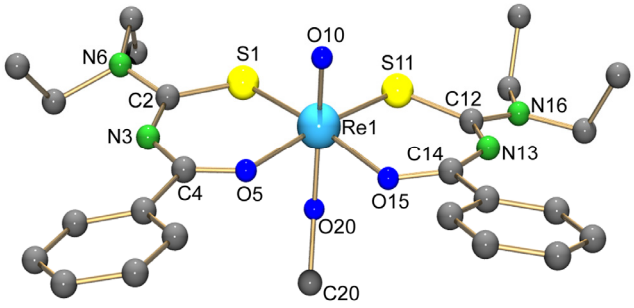

Figure 2.5 Molecular structure of [ReO(OMe)(Et_2btu)$_2$] (**3c**). Hydrogen atoms were omitted for clarity.

Table 2.4 Selected bond lengths in [ReO(OMe)(Et_2btu)$_2$] (**3c**)

Bond lengths (Å)					
Re–O10	1.699(5)	S1–C2	1.745(6)	S11–C12	1.757(5)
Re–S1	2.326(1)	C2–N3	1.345(7)	C12–N13	1.351(7)
Re–S11	2.321(1)	C2–N6	1.346(7)	C12–N16	1.335(6)
Re–O5	2.131(4)	N3–C4	1.313(7)	N13–C14	1.296(7)
Re–O15	2.129(3)	C4–O5	1.262(6)	C14–O15	1.266(6)
Re1–O20	1.795(7)				

Despite the ready formation of **3c** from **2c**, the methoxo ligand in **3c** is labile and can react with water finally to yield the oxo-bridged dimer [{ReO(Et_2btu)$_2$}$_2$O] (**4c**). The dimeric complex is formed when **3c** is dissolved in $CHCl_3$ or MeCN and a drop of water is added. This results in an immediate change of the colour from red to light green. Signals of **4c** are even observed during ^{1}H NMR measurements on **3c** in $CDCl_3$, when the solvent contains traces of water. On the other hand, the reaction is perfectly reversible and the green solution of **4c** in $CHCl_3$ suddenly turns to red when small amount of MeOH are added (Scheme 2.3). A corresponding ^{1}H-NMR experiment in $CDCl_3$ revealed that after the addition of 15 µl of MeOH the resonances of **4c** completely disappeared and complex **3c** is exclusively present in such solutions (Figure 2.6). A dimerization most probably occurs via formation of an intermediate hydroxo species [37,38], which has not been isolated in the present case. Remarkably, the equilibrium between **3c** and **4c** is completely reversible under common conditions. In most of the previous examples, the formation of the dimeric species is preferred [39,40]. Only in some exceptional cases, the cleavage of the Re–O–Re backbone of the $\{Re_2O_3\}^{4+}$ core has been used to prepare monomeric species, as in the synthesis of [ReO(OEt)Cl_2(py)$_2$] from [$Re_2O_3Cl_4$(py)$_4$] [37].

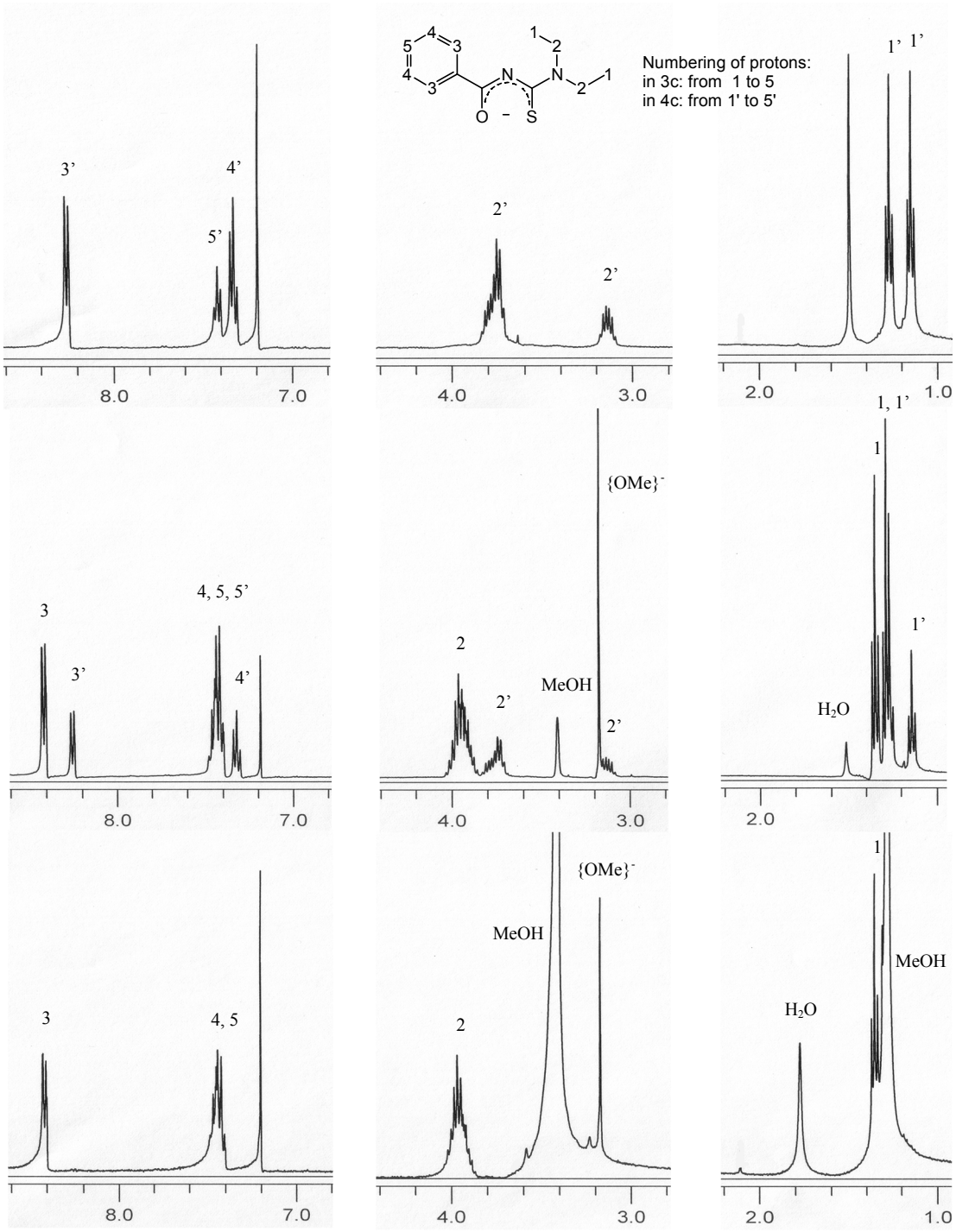

Figure 2.6 NMR spectra of a: [{ReO(Et$_2$btu)$_2$}$_2$O] (**4c**). b: [ReO(OMe)(R^{1}R^{2}btu)$_2$] (**3c)** in the present of a trace of H_2O. c: 20 mg of [{ReO(Et$_2$btu)$_2$}$_2$O] (**4c**) and 15 µl of MeOH.

The Re=O stretch in the IR spectrum of **4c** is only weak, which is in accord to previous reports on oxo-bridged dimer [39], and a strong absorption at 663 cm^{-1}, which is assigned to the asymmetric Re–O–Re stretch dominates. Each two sets of resonances are observed for the ethyl residues in **5c** and **6c** in the ^{1}H and ^{13}C NMR spectra due to the hindered rotation mentioned above, while only each one ^{13}C signal is observed for the carbon atoms of the chelate rings. This clearly indicates magnetic equivalence of the Et$_2$btu$^-$ ligands in these two

compounds. This is in accord with the structure of **3c** and strongly suggests a similar bonding situation in **4c**.

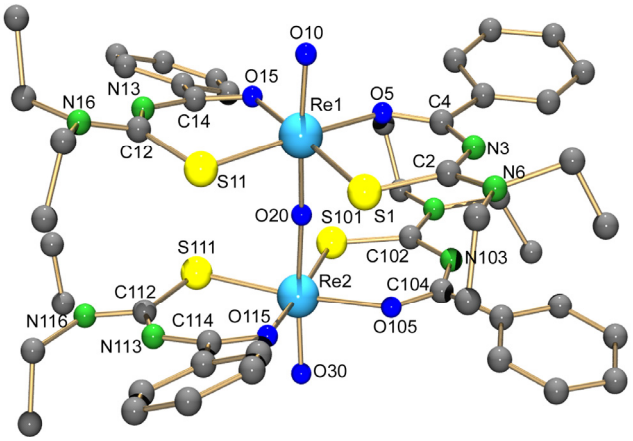

Figure 2.7 Molecular structure of $[\{ReO(Et_2btu)_2\}_2O]$ (**4c**). Hydrogen atoms were omitted for clarity.

Table 2.5 Selected bond lengths in $[\{ReO(Et_2btu)_2\}_2O]$ (**4c**)

Bond lengths (Å)			
Re–O10 / O20	1.703(7) / 1.687(8)	Re–O5 / O105	2.089(6) / 2.111(7)
Re–S1 / S101	2.340(3) / 2.325(3)	Re–O15 / O115	2.101(6) / 2.118(7)
Re–S11 / S111	2.334(3) / 2.334(3)	Re–O30 /Re11–O30	1.897(6) / 1.914(6)
S1–C2 / S101–C102	1.742(9) / 1.74(1)	S11–C12 / S111–C112	1.768(9) / 1.74(1)
C2–N3 / C102–N103	1.36(1) / 1.35(1)	C12–N13 / C112–N113	1.33(1) / 1.33(1)
C2–N6 / C102–N106	1.33(1) / 1.33(1)	C12–N16 / C112–N116	1.33(1) / 1.34(1)
N3–C4 / N103–C104	1.31(1) / 1.30(1)	N13–C14 / N113–C114	1.32(1) / 1.32(1)
C4–O5 / C104–O105	1.26(1) / 1.27(1)	C14–O15 / C114–O1115	1.27(1) / 1.27(1)

The spectroscopic results are confirmed by an X-ray structural analysis. Figure 2.7 illustrates the molecular structure of **4c**, selected bond lengths are contained in Table 2.5. The Re–O–Re unit is almost linear (169.9(3)°) and the corresponding bond lengths of 1.897(6) and 1.914(6) Å indicate some double bond character as has been found previously for other compounds with $\{Re_2O_3\}^{4+}$ core [33]. Expectedly (with regard to the NMR results), all chelate rings are almost planar and only negligible deviations (< 0.154 Å) are observed.

The structural diversity of the obtained rhenium compounds starting from common precursor complexes encouraged us to undertake similar experiments for technetium. Unfortunately, the analogous PPh_3 complex '$[TcOCl_3(PPh_3)_2]$' does not exist due to the ready reduction of $\{TcO\}^{3+}$ centers by monodentate phosphines [41]. Thus, reactions of $(NBu_4)[TcOCl_4]$ with HR^1R^2btu ligands were studied with methanol as solvent. They give yellow-brown, crystalline products of the composition $[TcOCl(R^1R^2btu)_2]$ (**5**) in good yields

(Scheme 2.5). The Tc compounds are much better soluble in MeOH than their rhenium analogues **1** and only small amounts of solvent may be used to obtain the products in good yields.

The IR spectra of **5** exhibit the $\nu_{(Tc=O)}$ frequencies in the range between 950 and 970 cm^{-1} and the spectral features described above for the analogous rhenium complexes **1**, such as the strong bathochromic shift of the C=O bands, also apply for the Tc compounds. The same holds true for the main structural characteristics. Figure 2.8 depicts the molecular structure of **5a** and selected bond lengths are listed in Table 2.6. Again, two chelate rings with different bonding characteristics are observed. An almost planar equatorial chelate ring (maximum deviation from the mean least square plane of all atoms of the chelate ring for atom Cl2: 0.201 Å) is accompanied by a strongly distorted ring in axial position.

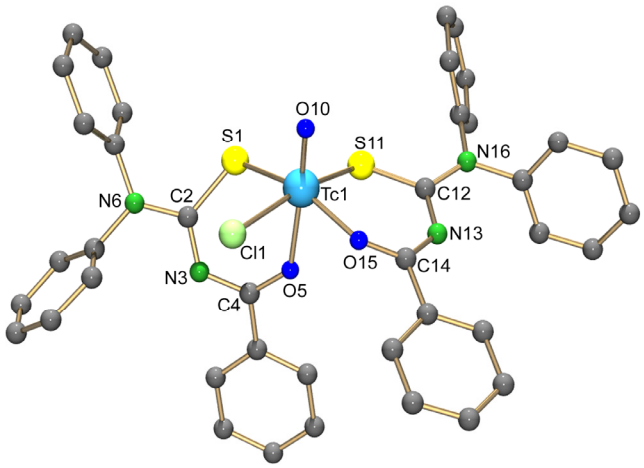

Figure 2.8 Molecular structure of $[TcOCl(Ph_2btu)_2]$ (**5a**). Hydrogen atoms were omitted for clarity.

Table 2.6 Selected bond lengths in $[TcO(Ph_2btu)_2]$ (**5a**)

Bond lengths (Å)					
Tc1–O10	1.642(4)	S1–C2	1.762(6)	S11–C12	1.750(5)
Tc1–S1	2.358(1)	C2–N3	1.320(7)	C12–N13	1.331(7)
Tc1–Cl1	2.437(2)	C2–N6	1.358(6)	C12–N16	1.352(7)
Tc1–S11	2.323(2)	N3–C4	1.364(6)	N13–C14	1.311(7)
Tc1–O5	2.147(3)	C4–O5	1.266(6)	C14–O15	1.285(6)
Tc1–O15	2.043(3)				

2.2.2 Re^{III} and Tc^{III} Complexes with Dialkylbenzoylthioureas

As mentioned above, $[ReCl_2(PPh_3)_2(R^1R^2btu)]$ (**6**) complexes were isolated from reactions of dialkylbenzoylthioureas and $[ReOCl_3(PPh_3)_2]$ in CH_2Cl_2 solutions as minor side-products together with the main products **1**. The formation of Re(III) complexes during such reactions is not unexpected and can be explained by the reduction of the Re(V) oxo complexes by the released PPh_3, which attacks the oxo ligands under formation of triphenylphosphine oxide. The presence of $OPPh_3$ in the reaction mixture is confirmed by its ^{31}P NMR signal. The mechanism of the reduction was first proposed by *Rouschias* and *Wilkinson* for the synthesis of $[ReCl_3(MeCN)(PPh_3)_2]$ [42], and more recently confirmed during reactions of $[ReOCl_3(PPh_3)_2]$ with other systems [43]. A dissociative mechanism with a trigonal-bipyramidal transition state is strongly suggested by the conformation of complexes **6** with the PPh_3 ligands in *trans* positions to each other and with respect of the bulky ligands of **1**.

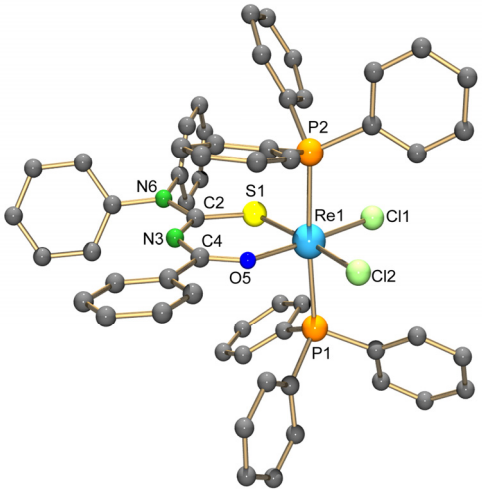

Figure 2.9 Molecular structure of $[ReCl_2(PPh_3)_2(Ph_2btu)]$ (**6a**). Hydrogen atoms were omitted for clarity.

Table 2.7 Selected bond lengths in $[ReCl_2(PPh_3)_2(Ph_2btu)]$ (**6a**)

Bond lengths (Å)					
Re–Cl1	2.389(1)	Re–O5	2.021(2)	C2–N6	1.364(4)
Re–Cl2	2.385(1)	Re–S1	2.360(1)	N3–C4	1.328(4)
Re–P1	2.486(1)	S1–C2	1.719(4)	C4–O5	1.270(4)
Re–P2	2.467(1)	C2–N3	1.341(5)		

In the infrared spectra of complexes **6,** the $\nu_{C=O}$ stretches are bathochromically shifted by about 200 cm^{-1} compared to those in non-coordinated benzoylthioureas. The bands in the region of 3100 cm^{-1} do not appear which indicates the expected deprotonation of the ligands during complex formation. No band in the region between 900 and 1000 cm^{-1}, which are

typical for $Re^{V}O$ complexes, can be found. The ^{1}H NMR spectra of the complexes **6** exhibit broad lines with unresolved peaks which are typical for paramagnetic Re(III) compounds. FAB^{+} mass spectra of **6** show peaks of the molecular ions and fragments, which result from subsequent loss of Cl^{-} and PPh_3.

A similar bonding situation as is described for **1a** is observed in the chelate ring of the rhenium(III) complex **6a**, but in contrast to **1e**, the C2–N6 bonds contribute to the conjugated π-system to a less extend and the chelate ring is almost planar with a maximum deviation from planarity of 0.04 Å for atom S1. Figure 2.9 depicts the molecular structure of **6a**, and selected bond lengths are contained in Table 2.7. The structure reveals a distorted octahedral environment of the rhenium atom with *trans* coordination of the bulky PPh_3 ligands. No unusual bond lengths are observed, the small differences to the structure of **1e** can be addressed to the different oxidation states of the rhenium atoms and/or the influence of the *trans* ligands.

The $\{TcO\}^{3+}$ core is much easier to be reduced than $\{ReO\}^{3+}$. Thus, the reactions of **5** with two equivalents of PPh_3 gives technetium(III) complexes very fast and even at room temperature. One equivalent of the phosphine is used as reducing agent and the formed $OPPh_3$ can readily be detected by ^{31}P NMR in the reaction mixture. The second equivalent is used for coordination in the resulting red $[TcCl(PPh_3)(R^1R^2btu)_2]$ complexes (**7**). The products are stable as solids and in solution. Figure 2.10 shows the molecular structure of **7a**. Selected bond lengths are contained in Table 2.8. The coordination sphere of the metal is best described as a distorted octahedron with *trans* angles between 172.9(1) and 177.7(1)°. Triphenylphospine coordinates *trans* to the oxygen atom of one of the Ph_2btu^{-} ligands. The chelate ring of this ligand is strongly distorted, while the second one is almost planar. The sulphur atoms are in *cis* position to each other.

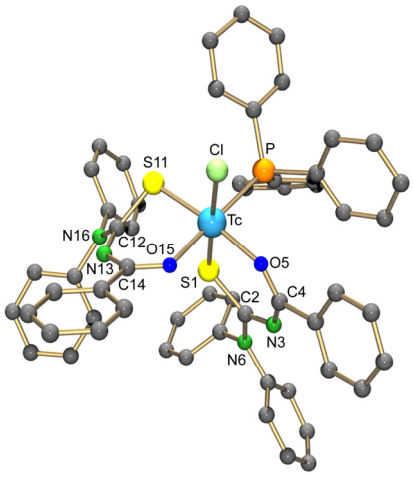

Figure 2.10 Molecular structure of $[TcCl(PPh_3)(Ph_2btu)_2]$ (**7a**). Hydrogen atoms were omitted for clarity.

Table 2.8. Selected bond lengths in $[TcCl(PPh_3)(Ph_2btu)_2]$ (**7a**)

Bond lengths (Å)			
Tc–Cl	2.417(2)	S1–C2 / S11–C12	1.726(8) / 1.723(8)
Tc–P	2.428(2)	C2–N3 / C12–N13	1.323(9) / 1.334(9)
Tc–S1 / S11	2.333(2) / 2.360(2)	C2–N6 /C12–N16	1.383(7) / 1.340(8)
Tc–O5 / O15	2.044(5) / 2.071(5)	N3–C4 / N13–C14	1.346(8) / 1.319(9)
		C4–O5 / C14–O15	1.257(7) / 1.280(8)

The chloro and PPh_3 ligands in the coordination sphere of **7a** are sufficiently labile to allow further ligand exchange. Thus, the reaction of **7a** with HPh_2btu in a CH_2Cl_2/MeOH mixture yields the dark red-brown tris-chelate $[Tc(Ph_2btu)_3]$ (**8a**) in good yields. The same product is formed in a one-pot reaction starting from **5a**, 3 equivalents of PPh_3 and an excess of HPh_2btu. In both cases, addition of a base such as Et_3N supports deprotonation of the N,N-dialkylbenzoylthiourea and, thus, the formation of the chelate complex. An alternative synthesis of compounds of the type **8** has been described previously starting directly from pertechnetate with $SnCl_2$ as reducing agent [31]. This procedure, however, produced a mixture of compounds and a chromatographic purification was necessary, while the present ligand exchange approach gives **8** with high purity and in crystalline form.

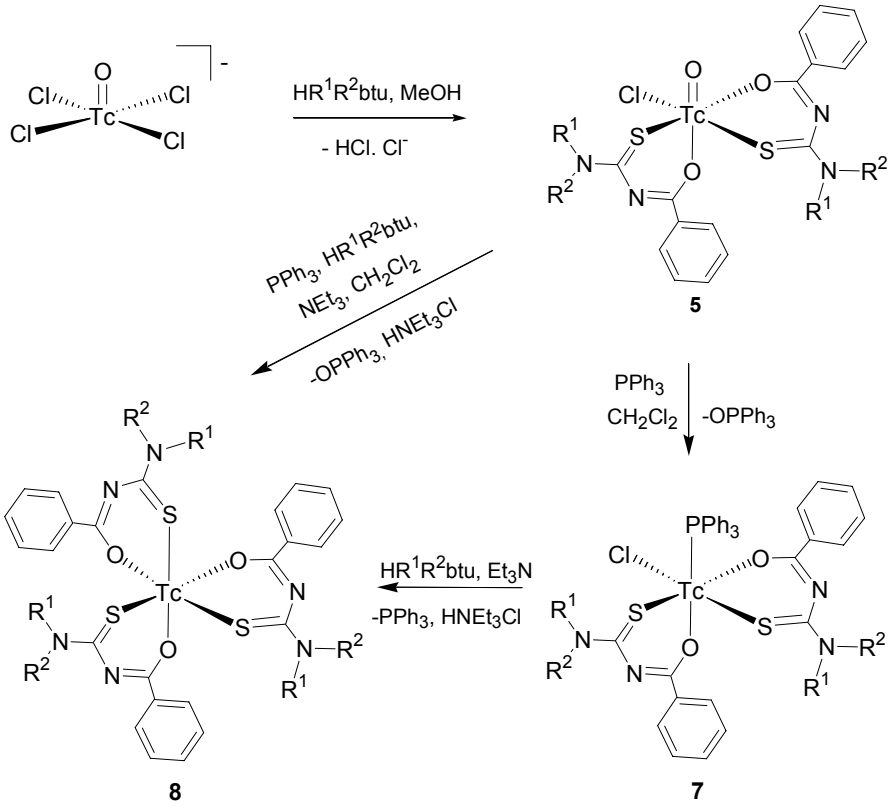

Scheme 2.5 Synthesis of $[TcOCl(R^1R^2btu)_2]$ (**5**), $[TcCl(PPh_3)(Ph_2btu)_2]$ (**7a**) and $[Tc(Ph_2btu)_3]$ (**8a**).

Figure 2.11 illustrates the molecular structure of complex **8a**. It shows only minor deviations from idealized octahedral geometry with *trans* angles in the range 174.4(1)-176.0(1)^{o}. The distorted octahedral geometry is defined by two sets of three facially bound sulphur and oxygen atoms from three Ph_2btu^- ligands. All chelate rings in **8a** are almost planar. The O-Tc-O bond angles fall in the range 84.5(2) - 86.3(2) which is slightly smaller than the S-Tc-S bond angles (90.4(1) - 91.1(1)). Similar patterns have been observed previously for the tris-chelates *fac*-[$Ru(Et_2btu)_3$], *fac*-[$Rh(Et_2btu)_3$], *fac*-[$Co(Et_2btu)_3$] and *fac*-[$Co(Morphbtu)_3$] [30].

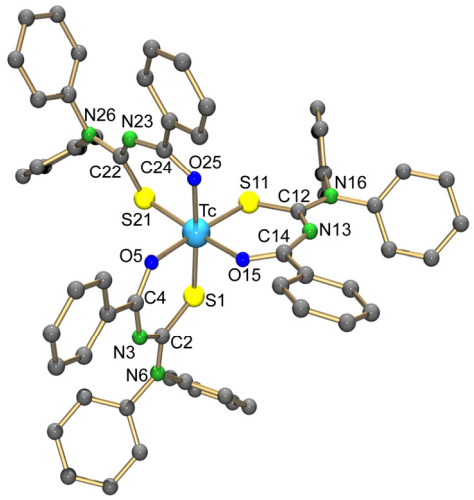

Figure 2.11 Molecular structure of [$Tc(Ph_2btu)_3$] (**8a**). Hydrogen atoms were omitted for clarity.

Table 2.9 Selected bond lengths in [$Tc(Ph_2btu)_3$] (**8a**)

Bond lengths (Å)	
Tc–S1 / S11 / S21	2.340(1) / 2.352(1) / 2.343(2)
Tc–O5 / O15 / O25	2.049(3) / 2.046(4) / 2.048(4)
S1–C2 / S11–C12 / S21–C22	1.735(6) / 1.738(6) / 1.738(6)
C2–N3 / C12–N13 / C22–N23	1.329(7) / 1.323(7) / 1.337(8)
C2–N6 /C12–N16 / C22–N26	1.370(7) / 1.371(6) / 1.355(7)
N3–C4 / N13–C14 / C23–C24	1.333(7) / 1.327(6) / 1.330(7)
C4–O5 / C14–O15 / C24–O25	1.266(6) / 1.273(6) / 1.278(6)

2.2.3. Re^{V}(NPh) Complexes with Dialkylbenzoylthioureas

The phenylimido and the oxo cores of rhenium(V) complexes, $[Re{=}NPh]^{3+}$ and $[Re{=}O]^{3+}$, are chemically very similar [33]. This has been demonstrated by the synthesis of a number of

structurally analogous complexes, including the triphenylphosphine complexes $[ReOX_3(PPh_3)_2]$ (X = Cl, Br) and $[Re(NPh)X_3(PPh_3)_2]$ (X = Cl, Br, I). Both are used as common precursors in the synthesis of Re(V) oxo and Re(V) phenylimido complexes by ligand exchange reactions [33,44]. Reactions of HR^1R^2btu with these two starting materials, however, showed a different course of the reactions. At ambient conditions, in CH_2Cl_2 or acetone, $[ReOCl_3(PPh_3)_2]$ readily reacts with HR^1R^2btu under formation of different products, while the phenylimido complex $[Re(NPh)Cl_3(PPh_3)_2]$ does not react. Prolonged heating on reflux in CH_2Cl_2 and the addition of NEt_3 as a supporting base resulted in the gradual consumption of $[Re(NPh)Cl_3(PPh_3)_2]$, but results in the formation of intractable brown solutions. Unfortunately, all our attempts to isolate crystalline product from the reactions of this precursor failed.

More successful were reactions using another Re(V) phenylimido precursor, $[Re(NPh)Br_3(PPh_3)_2]$. The bromo derivative quickly reacts with the corresponding benzoylthioureas in warm CH_2Cl_2 under formation of $[Re(NPh)Br_2(Ph_2btu)(PPh_3)]$ (**9a**) and $[Re(NPh)Br_2(Morphbtu)(PPh_3)]$ (**9e**). The yellow-green solids can be isolated in good yields from the yellow-green solutions as the sole products. No further reduction of the products was found. This comes not completely unexpected, since the formation of rhenium(III) side products during ligand exchange reactions starting from $[ReOCl_3(PPh_3)_2]$ is commonly explained by an attack of released PPh_3 to the oxo ligand with subsequent formation of $OPPh_3$ and reduction of the metal ion. This is certainly not possible with the phenylimido species under study. An additional stabilization of the higher oxidation state might be given by the fact that the nitrogen atom is a stronger π electron donator and a weaker electron acceptor than the oxygen atom as has been discussed recently [45]. Experimental support for this discussion is given by ^{31}P-NMR spectra of reaction mixtures, which show the presence of a considerable amount of $OPPh_3$ in the reaction mixture of the oxo compounds, while only the signals of the $[Re(NPh)Br_2(R^1R^2btu)(PPh_3)]$ complexes and released PPh_3 could be detected for the reactions of phenylimido complexes.

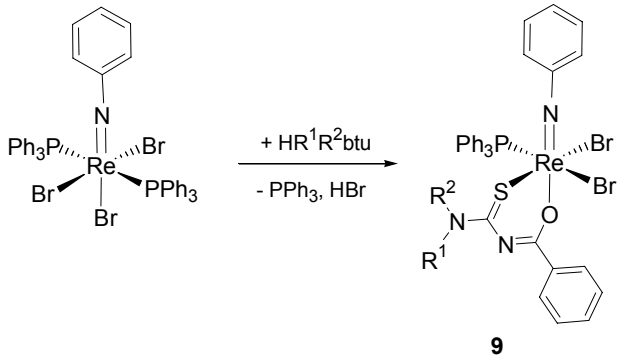

9

Scheme 2.6 Reaction of HR^1R^2btu and $[Re(NPh)Br_3(PPh_3)_2]$.

The infrared spectra of the imido compounds are very similar to those of the oxo complexes. All exhibit strong bands between 1470 and 1510 cm^{-1} which are assigned to the $\nu_{C=O}$ vibrations. This corresponds to a strong bathochromic shift of approximately 200 cm^{-1} and indicates chelate formation with a large degree of electron delocalization within the chelate rings [16]. The absence of ν_{NH} bands in the region of 3100 cm^{-1} indicates the expected deprotonation of the ligands. The Re=N vibrations can not be assigned unambiguously in the IR spectra of **9a** and **9e**. The FAB^+ mass spectrum of the phenylimido complex **9a** shows an intense signal for the molecular ions at m/z = 1032 with the expected isotope distribution.

NMR spectra of the compounds **9** reflect the hindered rotation around the C–NR^1R^2 bonds. This leads to complex coupling patterns in the proton spectra as in that of **9e**, where the CH_2 protons show a complex array of overlapping multiplets in the range between 3.8 and 4.7 ppm. The signals of the C=O carbon atoms in **9** appear in the region of 190 ppm which well agrees with the corresponding chemical shift detected in the ^{13}C-NMR spectrum of **1**. The coordination of triphenylphosphine in **9** is confirmed by ^{31}P NMR resonances between 1.0 and 1.8 ppm.

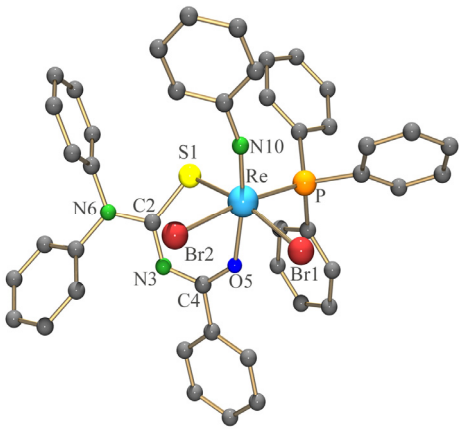

Figure 2.12 Molecular structure of [Re(NPh)Br_2(Ph_2btu)(PPh_3)] (**9a**). Hydrogen atoms were omitted for clarity.

Table 2.10 Selected bond lengths in [Re(NPh)Br_2(Ph_2btu)(PPh_3)] (**9a**)

Bond lengths (Å)					
Re1– N10	1.725(6)	Re1–S1	2.415(2)	C2–N3	1.316(9)
Re1–P1	2.422(2)	Re1–O5	2.064(4)	N3–C4	1.322(9)
Re1– Br1	2.535(1)	S1–C2	1.749(6)	C4–O5	1.283(8)
Re1– Br2	2.605(1)	C2–N6	1.363(8)	N10–C61	1.366(9)

Figure 2.12 depicts the molecular structure of **9a**. Selected bond lengths are shown in Table 2.10. The rhenium atom is found in a distorted octahedral coordination environment. The axial positions are occupied by the oxygen atoms of the chelating ligands and the double bonded nitrogen atoms of the phenylimido ligand. The equatorial plane is formed by the

sulphur atoms of the singly deprotonated benzoylthiourea, the phosphorus atom and the two bromo ligands, which are in *cis* arrangement to each other. The rhenium atom is located above the mean least-squared plane formed by the equatorial donor atoms by 0.194 Å towards the Re=N double bond. The Re=N distance of 1.725(6) Å in **9a** is slightly shorter with respect to some other Re(V) phenylimido complexes having an oxygen atom coordinated *trans* to a NPh^{2-} ligand [46].

2.3 A Rhenium Complex with N-Picolylbenzoylthiourea

Generally, structures of H_2Rbtu are characterized by the strong intramolecular hydrogen bonds established between the thiourea C(S)NHR moiety and the oxygen atom of the amidic group and 'lock' the C(O)NHC(S)NHR unit into a planar six-membered ring [17] (see also Scheme 2.7). This intramolecular hydrogen bond, results in substantial differences in the preferred conformation of H_2Rbtu compared to the twisted conformation of HR^1R^2btu [47], with the sulphur and oxygen atoms being located in opposite directions, which consequently results in difference in the coordination chemistry. By the fact the H_2Rbtu ligands mainly act as neutral, monodentate ligands and coordinate to metal ions via their sulfur donor atoms. This coordination fashion is found in few complexes with Pt^{2+}, Pd^{2+}, Hg^{2+} and Cu^{2+} ions [48].

In the solid state of H_2picbtu, the intramolecular hydrogen bond N6-H6...O5 is also found (see Figure 2.1 and Scheme 2.7) and suggests that the compound may serve as a tridentate ligand via the atoms O5, N6 and N46. However, the reaction of H_2picbtu with $(NBu_4)[ReOCl_4]$ in acetone yields a green solid of the composition $(NBu_4)_2[\{Re_2O_2Cl_5(Hpicbtu)\}_2O]$ (**10**). Single crystals of the compound are instable at room temperature and readily form a green powder by the loss of solvent acetone. The complex is almost insoluble in most common solvents and only sparingly soluble in warm DMSO, where a subsequent decomposition is observed, which goes along with a color change to purple.

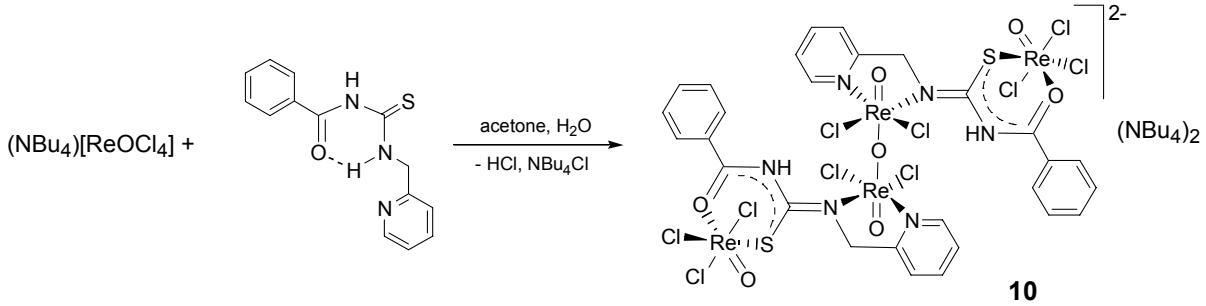

Scheme 2.7 Reaction of H_2picbtu with $(NBu_4)[ReOCl_4]$.

The IR spectrum of the compound exhibits a sharp, medium absorption at 3291 cm^{-1} corresponding to the NH vibration and a very strong absorption band at 1635 cm^{-1} can be assigned to the C=O stretch. The position of this band indicates only a slight bathochromic shift with respect to the non-coordinated H_2picbtu. This is a significantly difference to the spectra which were obtained for N,N-dialkyl-N'-benzoylthioureas and their rhenium complexes, where strong bathochromic shifts of the C=O bands in the spectra of the complexes were indicative for extended π-systems. The Re=O vibration in $(NBu_4)_2[\{Re_2O_2Cl_5(Hpicbtu)\}_2O]$ appears as a strong band at 991 cm^{-1}, which is in the expected range [33].

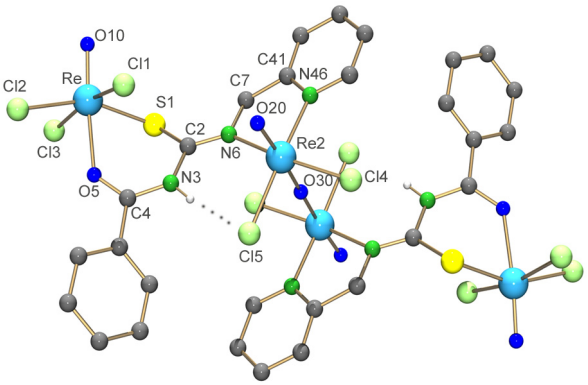

Figure 2.13 Structure of the complex anion of $(NBu_4)_2[\{Re_2O_2Cl_5(Hpicbtu)\}_2O]$ **10**. Hydrogen bond: N3-H3: 0.86 Å, Cl5…H2: 2.239 Å, N3…Cl5: 3.092(2), N3-H3-Cl5: 171.6°. Hydrogen atoms bonded to carbon atoms were omitted for clarity.

Table 2.11 Selected bond lengths in $(NBu_4)_2[\{Re_2O_2Cl_5(Hpicbtu)\}_2O]$ (**10**)

Bond lengths (Å)					
Re1–O10	1.644(6)	Re2–O20	1.697(6)	S1–C2	1.759(7)
Re1–Cl1	2.365(2)	Re2–Cl4	2.383(2)	C2–N3	1.387(9)
Re1–Cl2	2.348(2)	Re2–Cl5	2.416(2)	N3–C4	1.347(9)
Re1–Cl3	2.380(2)	Re2–N6	2.169(5)	C4–O5	1.251(8)
Re1–S1	2.352(2)	Re2–N46	2.123(7)	C2–N6	1.276(9)
Re1–O5	2.227(5)	Re2–O30	1.912(1)	N6–C7	1.474(10)

Figure 2.13 illustrates the tetrameric structure of the complex anion. Selected bond lengths are given in Table 2.11. The benzoylthiourea is singly deprotonated and binds to two different rhenium atoms. One rhenium atom coordinates to the ligand via the atoms S1 and O5 and, thus, forms a common S,O chelate as has previously been observed for many N,N-dialkyl-N'-benzoylthioura complexes, while the second rhenium atom binds to the pyridine and (monoalkyl)amine nitrogen atoms N6 and N46, respectively. The Re-S distance of 2.352(2) Å and the C2-S1 bond length of 1.759(7) Å, which is 0.083 Å longer than in H_2picbtu, fall in the range of those in other oxorhenium(V) benzoylthiourea complexes.

A remarkably long bond of 2.227(5) Å is observed for the Re1-O5 bond. This is at the upper limit of *trans*-O=Re-O single bond distances in Re(V) oxo complexes. Similar values have previously only been reported for some complexes with small monodentate neutral ligands such as H_2O, MeOH or Me_2CO [49], while all previously reported Re-O bond lengths in corresponding benzoylthioureato complexes are shorter (2.068 Å – 2.098 Å). Another remarkable structural feature in **10** is the short C4-O5 distance of 1.251(8) Å. This is shorter than corresponding distances in almost all benzoylthioureato chelates. It is, however, consistent with the observed high frequency of the $\nu_{C=O}$ stretch in the IR spectrum and indicates an almost isolated C=O double bond. Despite the fact that the nitrogen atom N3 remains protonated and the corresponding hydrogen atom H3 forms an intramolecular hydrogen bond to Cl5, the C-N bonds in the chelate ring show partial double bond character with bond lengths of 1.387(9) Å and 1.347(9) Å. This can be understood by a significant transfer of electron density from the neighboring chelate ring to the S,O chelate of rhenium atom Re1.

The almost planar environment of the atom N6 suggests the deprotonation of the N6-H group. The short N6-C2 bond in **10**, which is in the range of C=N double bonds, is without precedence in the coordination chemistry of benzoylthioureas. This, however, allows a transfer of electron density into the chelate ring of the neighboring rhenium atom (*vide supra*).

The unusual distribution of electron density between the two chelate rings may also explain the condensation of two of the dimeric complex units under final formation of the tetrameric anion via a μ-oxo ligand. Principally, the formation of dimeric rhenium(V) complexes with the linear $\{O=Re-O-Re=O\}^{4+}$ core is not uncommon and the Cambridge structural database contains 98 entries with this structural feature. However, complex **10** is beside the cyano complex $[\{ReO(CN)_4\}_2O]^{4-}$ only the second example of a complex anion with a linear oxo bridge [50], while commonly the formation of μ-oxo ligands is established for charge compensation in cationic intermediates [33,51]. This may support the discussion above and underline the exceptional properties of N-monoalkyl-N'-benzoylthioureas, which allows a fine-tuning of the electron distribution between the metal atoms in binuclear complexes.

2.4 Rhenium Complexes with N-Aroylbis(N,N-dialkylthioureas)

Surprisingly, the chelating complexes of $H_2dpic(R^1R^2tu)_2$ have not been reported yet. Hitherto, only one silver (I) complex of $H_2dpic(R^1R^2tu)_2$ in which the ligand act as unidentate simple thioureas was published [19]. In contrast, the coordination chemistry of $H_2phth(R^1R^2tu)_2$ ligands with several transition ions like Cu^{2+}, Ni^{2+}, Pd^{2+} and Pt^{2+} is well documented [18,52]. All well characterized structures belong to the *cis* square-planar binuclear fashion, in which each aroylthiourea side in $H_2phth(R^1R^2tu)_2$ acts as a bidentate monoanionic ligand like HR^1R^2btu. [52] The binuclear complexes of metal ions which can adopt octahedral geometry by the addition of ligands in the axial positions like Ni^{2+}, can be polymerized by treatment of exo-bidonor linkers such as: pyrazine, 4,4'-bipyridine, 1,2-di(4-pyridyl)ethane or 1,2-di(4-pyridyl)ethylene [53].

2.4.1 Rhenium Complexes with *m*-Phthaloylbis(N,N-dialkylthioureas)

The manifold of the coordination chemistry of rhenium and technetium with bidentate benzoylthioureas was the motivation to extend these studies for *m*-phthaloylbis(N,N-dialkylthioureas) - $H_2phth(R_2tu)_2$ which should be particularly suitable for the formation of binuclear planar rhenium methoxo complexes. Thus, the reaction of $H_2phth(R^1R^2tu)_2$ and $(NBu_4)[ReOCl_4]$ was undertaken in refluxing MeOH with the addition of Et_3N. Such reactions gave red solids with the composition $[(ReO(OMe)\{phth(R^1R^2tu)_2\})_2]$ (**11**) in high yields.

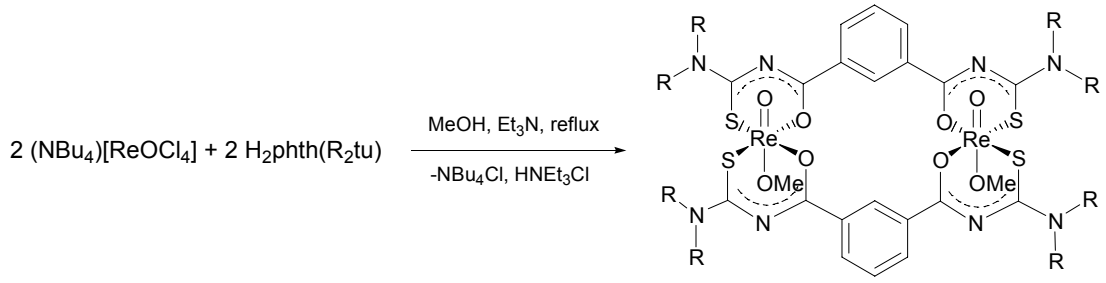

11

Scheme 2.8 Reaction of $H_2phth(R^1R^2tu)_2$ with $(NBu_4)[ReOCl_4]$.

IR spectra of **11** show the absence of absorptions in the region above 3100 cm^{-1} and reveals a strong shift of the C=O stretch band to the 1500 cm^{-1} region. This indicates the deprotonation and chelate formation of the organic ligand. The absorption band of the Re=O vibration is observed in the range between 940 cm^{-1} and 945 cm^{-1}, which is in the same region as in the methoxo complex **3c**.

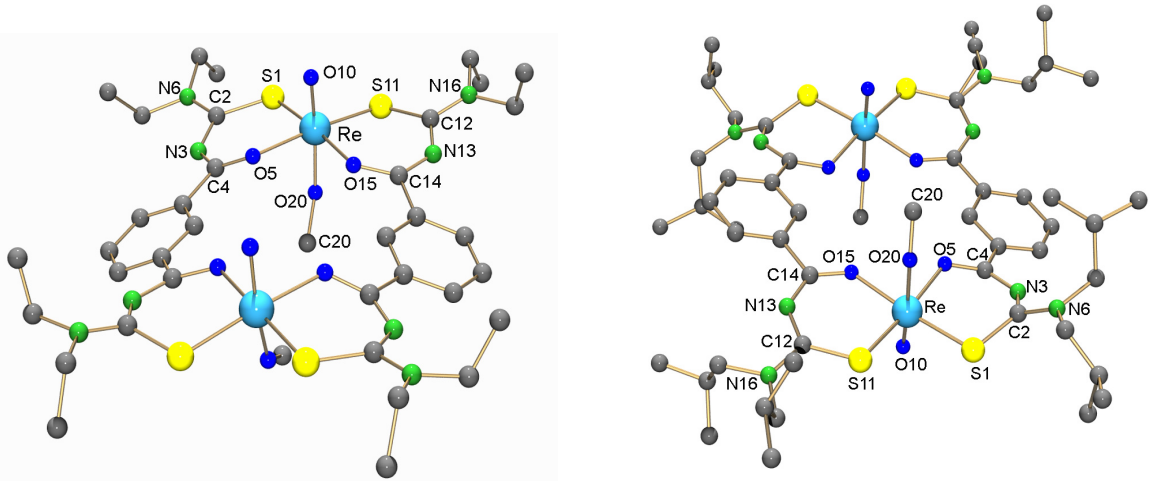

Figure 2.14 Molecular structure of [{ReO(OMe)phth(Et_2tu)$_2$}$_2$] **(11a)** and [{ReO(OMe)Phth(i-Bu_2tu)$_2$}$_2$] **(11b)**. Hydrogen atoms were omitted for clarity.

Table 2.12 Selected bond lengths in **(11a)** and **(11b)**

	11a	**11b**		**11a**	**11b**
Re–O10	1.699(6)	1.701(8)	C2–N6	1.333(9)	1.33(1)
Re–O20	1.881(6)	1.871(7)	N3–C4	1.313(9)	1.31(1)
Re–S1	2.343(2)	2.324(2)	C4–O5	1.267(8)	1.27(1)
Re–S11	2.336(2)	2.320(2)	S11–C12	1.747(8)	1.778(9)
Re–O5	2.112(5)	2.138(6)	C12–N16	1.350(9)	1.31(1)
Re–O15	2.111(5)	2.117(6)	C12–N13	1.343(9)	1.35(1)
S1–C2	1.747(8)	1.746(9)	N13–C14	1.313(9)	1.32(1)
C2–N3	1.339(9)	1.36(1)	C14–O15	1.264(9)	1.29(1)

Good quality single crystals of **11** are obtained by slow evaporation of their CH_2Cl_2 – MeOH solutions. Molecular structures of the products were studied by single crystal X-ray diffraction. Figure 2.14 depicts the molecular structures of **11a** and **11b**. Selected bond lengths are compared in Table 2.12. Both compounds exhibit binuclear structures each containing two H_2Phth(R_2tu)$_2$ ligands in which each organic ligand H_2phth(R_2tu)$_2$ forms two aroylthiourea chelates with two rhenium centers in the equatorial plane. The octahedral environment of the rhenium centers is completed by each an oxo ligand and a methoxo ligand, which are placed in axial positions. Thus, the coordination fashion of each rhenium atom is similar to that discussed for **3c**. Two coordination sites in the complexes **11a** and **11b** each are symmetry related. However, while the symmetry element in **11a** is a glide with the transformation element (-x, y, 1.5-z), the rhenium atoms in **11b** are related with a inversion symmetry (2-x, 1-y, 1-z). These two different symmetry elements consequently result in different orientation of the axial coordination units within the dimeric units. Thus, compound

11a has two methoxo ligands at the same side of the equatorial plane (*syn* isomer), in **11b** the methoxo ligands are in opposite directions (*anti* isomer). Bond lengths observed in **11** are similar to those discussed for **3c**. The Re-O10 bond lengths of 1.699(6) Å in **11a** and 1.701(8) Å in **11b** are in the typical range of rhenium oxygen double bonds [33]. The Re-O20 bond distances fall in the range between 1.871(7) Å and 1.881(6) Å reflecting considerable double bond character, which is transported from Re-O10 double bond to the *trans* axial position.

The methoxo complexes **11** are readily soluble in chlorinated solvents such as CH_2Cl_2 or $CHCl_3$ but sparingly soluble in alcohols, acetone or acetonitrile. In solutions, these complexes are only stable in the presence of a small amount of MeOH. When MeOH is not added, the solutions of **11** slowly change their color from red to green and give precipitates, which are no more soluble in organic solvents. The green compounds cannot be re-converted into the red complexes by addition of MeOH and heating as has been previous demonstrated for **3c**. Thus, recrystallization of compounds **11** from CH_2Cl_2 – MeCN solutions gave a mixture of green crystals of the composition $[(\{ReOphth(R^1R^2tu)_2\}_2O)_2]$ (**12**) and a fine green powder (**12^n**). The IR spectra of both products show very less intense absorptions of Re=O stretches around 915 cm^{-1} and one additional strong absorption at the region between 655 cm^{-1} and 585 cm^{-1} which is typical for asymmetric Re–O–Re stretches in oxygen bridging rhenium(V) compounds. As the case of **3c**, we can suppose that in the solution, compounds **11** are hydrolysed by traces of water and then are condensed under formation of the oxygen bridged complexes **12** and **12^n**.

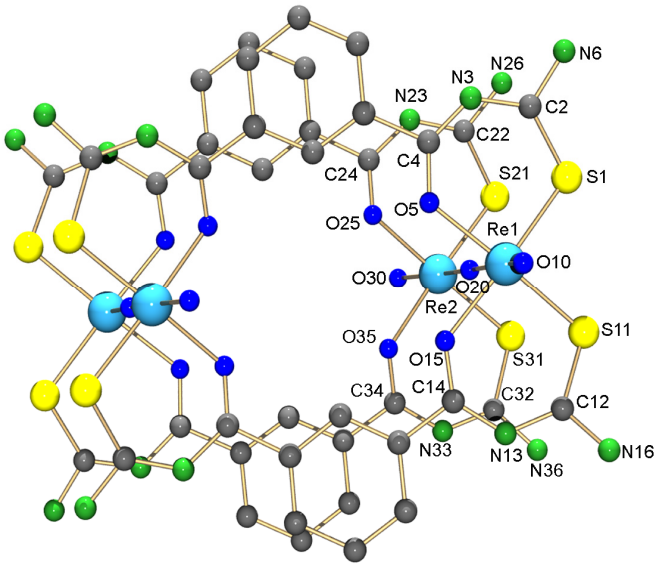

Figure 2.15 Molecular structure of $[(\{ReOphth(R^1R^2tu)_2\}_2O)_2]$ (**12**). Terminal alkyl groups and hydrogen atoms were omitted for clarity.

Table 2.13 Selected bond lengths (Å) in $[(\{ReOphth(R^1R^2tu)_2\}_2O)_2]$ (**12**)

	12a	**12b**		**12a**	**12b**
Bond lengths (Å)					
Re1–O10	1.690(9)	1.68(1)	Re2–O30	1.698(9)	1.70(1)
Re1–O20	1.905(9)	1.90(1)	Re2–O20	1.903(9)	1.91(1)
Re1–S1	2.317(4)	2.330(4)	Re2–S21	2.344(4)	2.372(5)
Re1–O15	2.143(9)	2.15(1)	Re2–O35	2.121(9)	2.07(1)
Re1–S11	2.324(4)	2.304(4)	Re2–S31	2.340(4)	2.391(5)
Re1–O5	2.148(9)	2.166(9)	Re2–O25	2.114(9)	2.10(1)

Interestingly, the ratio of compounds **12** and **12^n** obtained by recrystallization from CH_2Cl_2 – MeCN solutions is changed when the concentration of **11** is changed. Particularly, when starting from a highly diluted solution of **11** and slow recrystallization, bigger amounts of compounds **12** can be isolated. Figure 2.15 illustrates the skeleton molecular structure of **12**. The selected bond lengths of **12a** and **12b** are compared in Table 2.13. Compounds **12** reveal a tetranuclear structure containing two dimeric blocks which are equivalent and generated from the other by the symmetry transformation : (2 - x, 1 - y, 1 - z). It is clear that compound **12a** is formed from hydrolytic dimerization of the syn isomer **11a**. A similar reaction has previously been described for the formation of **4c** from **3c**. However, the formation of **12b** from **11b** is unexpected, since **11b** is an anti isomer which should be suitable to form a chain polymer or oligomer but not a discrete tetrameric molecule. This means, compound **12b** must be formed from the *syn* isomer of **11b**. This strongly suggests that both compounds **11** consist of a mixture of *syn* and *anti* isomers, even when their crystals look absolutely unique with respect to color and shape. Many attempts to find one crystal having a different cell dimension and structure failed.

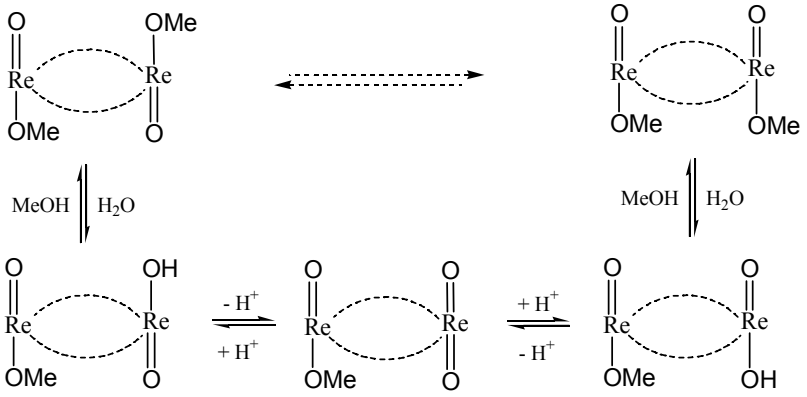

Scheme 2.9 Proposed mechanism for reversible transformation between *syn* and *anti* isomer of **11** in the solution.

The results discussed above, however, fit with NMR studies. ^{1}H NMR spectra of freshly prepared samples of **11** in $CDCl_3$ show two series of signals with the ratio approximately 0.80 : 1.00 and 0.70 : 1.00 respectively for **11a** and **11b**, each of which can be attributed to one symmetry-isomer of the binuclear methoxo complexes and a trace of signals belongs to a hydrolysed product (Figure 2.16). In order to prevent the hydrolysis of **11** and further condensation, 0.1 mL of MeOH-d_4 was added. Under such condition, the signals, which belong to hydrolysed products, almost disappeared. This reflects that the hydrolysis and the methanolysis of **11** are in an equilibrium (Scheme 2.9). Because of the exchange with the MeOH-d_4 solvent, the methoxo signals are less resoluble and appear as a broad multiplet signal at 3.36 ppm. However, two series of aromatic resonances with the unchanged ratio are remained. It is clear that the hindered rotation of NR_2 can lead to the magnetic difference between two alkyl residues, but will not change the chemical shifts of aromatic protons and methoxo groups. Nevertheless, the pattern obtained from ^{1}H NMR of **11** can be explained when it is assumed that both *anti* and *syn* isomers of **11** are presented. More interestingly, the ratio of two isomers in the solution is not significantly changed during hydrolysis or crystallization but only changes a little to 0.65: 1.00 determined by ^{1}H NMR for compound **11a** at -70 ^{o}C. This reveals an equilibrium between two *anti* and *syn* isomers. The mechanism of the equilibrium is proposed in Scheme 2.9.

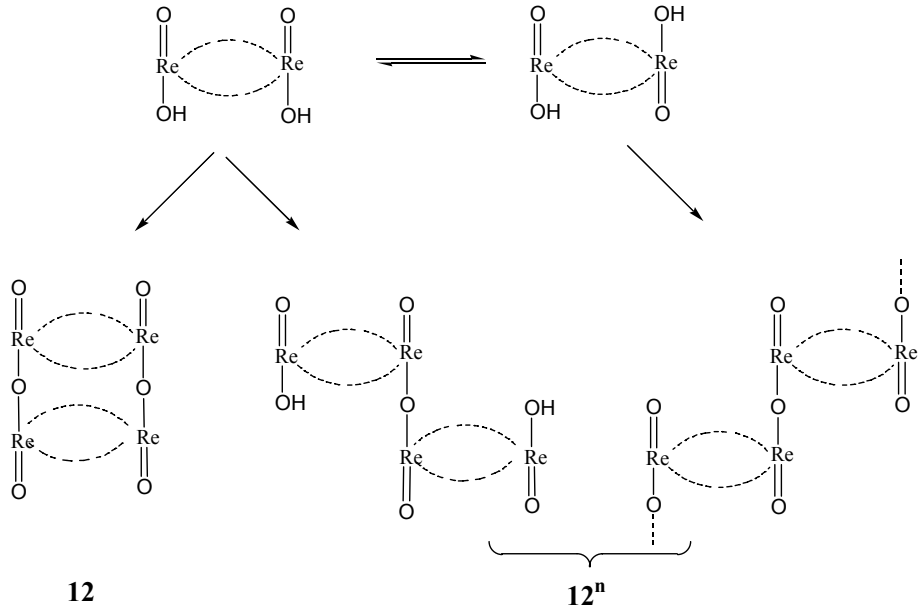

Scheme 2.10 Formation of tetranuclear complex **12** and the oligomeric compound **12^n**.

The discussion above underlines that in the solution both *anti* and *syn* isomers of **11** are present and can convert into each other. In the solid state, the compounds **11** exist as the isomer which has the higher lattice energy. This is the *syn* isomer for **11a** and the *anti* isomer

for **11b**. Consequently, the equilibrium of *anti* and *syn* isomers of the hydroxo complexes, which are intermediately formed from **11** should be considered. However, the condensation of hydroxo species and the formation of oxo-bridged compounds are chemically irreversible. This may be the main reason for the different ratios between the crystalline compounds **12** and the fine powders $\mathbf{12^n}$ and that they vary with the conditions of recrystallization. Beside the tetranuclear compound **12**, also other dimeric, oligomeric or polymeric species may be formed from **11** and are assigned for $\mathbf{12^n}$ (Scheme 2.10).

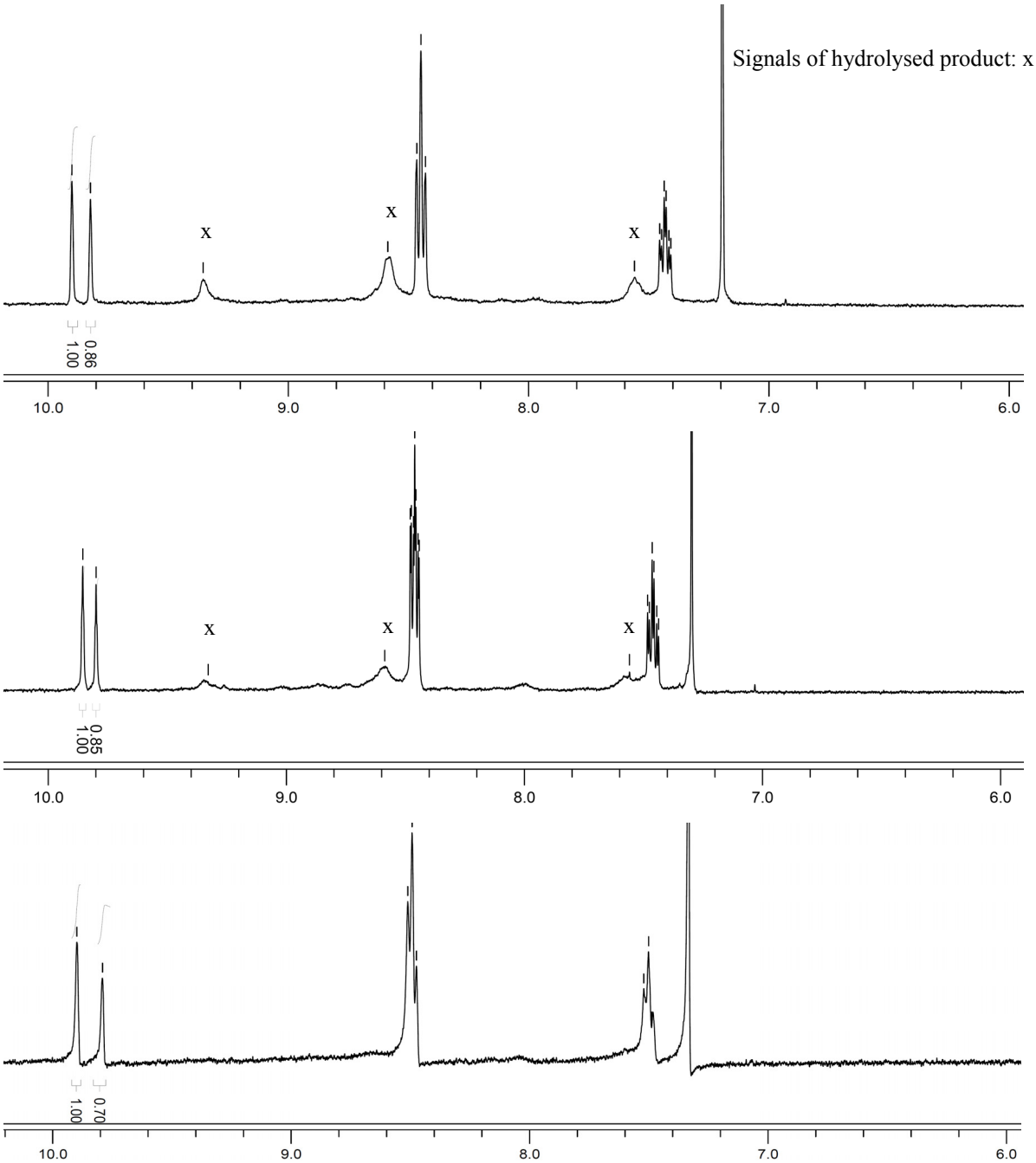

Figure 2.16 NMR spectra of a: **11a** in $CDCl_3$ at 20 °C, b: **11a** in $CDCl_3$ with 0.1 mL MeOD-d_4 at 20 °C, c: **11a** in $CDCl_3$ with 0.1 mL MeOD-d_4 at -70 °C.

2.4.2 A Rhenium Complexes with 2,6-Dipicolinoylbis(N,N-diisobutylthiourea)

Based on the chemical structure of H_2dpic(*i*-Bu_2tu)$_2$ we could expect that the coordination behaviour of this ligand toward rhenium will be mostly the same like that of H_2phth(R^1R^2tu)$_2$ or at least similar to that of HR^1R^2btu ligands. However, the reaction of H_2dpic(*i*-Bu_2tu)$_2$ with (NBu_4)[$ReOCl_4$] in MeOH solution results in a hitherto unprecedented coordination mode of benzoylthioureas (Scheme 2.11).

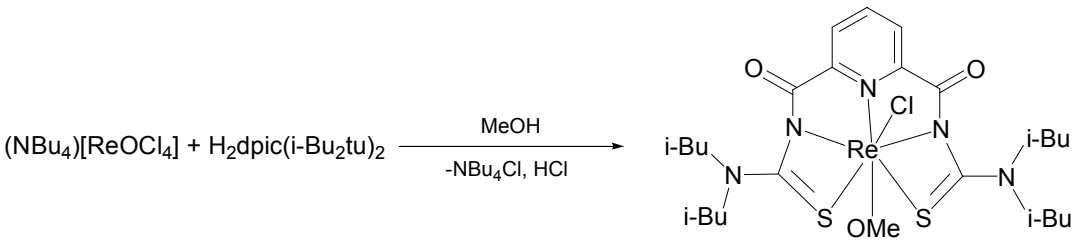

Scheme 2.11 Reaction of H_2dpic(i-Bu_2tu)$_2$ with (NBu_4)[$ReOCl_4$].

After addition of the ligand to a solution of (NBu_4)[$ReOCl_4$] in MeOH, the color of the mixture immediately turned to almost black. No solid precipitated even after reflux and the addition of base. The black powder, which was obtained after complete removal of the solvent, is sparingly soluble in diethyl ether. Slow evaporation of such a solution gave black crystals of the composition [ReCl(OMe){dpic(*i*-Bu_2tu)$_2$}] (**13**).

The IR spectrum of **13** shows an intense absorption corresponding to the C=O stretch at 1655 cm^{-1} which is even higher than the wave number of that stretch in **10,** where H_2picbtu coordinated as a neutral ligand and in the same range of S-monodentate coordinated HR^1R^2btu ligands [17]. The intense band at the region between 900 – 1000 cm^{-1} which normally assigned to a Re=O vibration is not present in IR spectrum of **13**. The ^{1}H NMR of **13** reveals broad signals and indicates its paramagnetism. The mass spectrum of **13** shows the expected molecular peak $[M + H]^+$ for a composition of [ReCl(OMe){dpic(*i*-Bu_2tu)$_2$}] at 758.1947 (the calculated value is 758.1975).

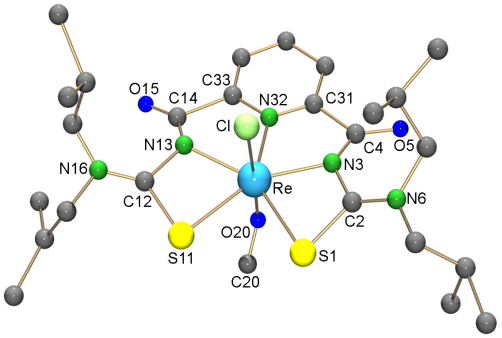

Figure 2.17 Molecular structure of [ReCl(OMe){dpic(*i*-Bu_2tu)$_2$ }] (**13**). Hydrogen atoms were omitted for clarity.

The compound **13** crystallizes in very thin crystals. The data set collected from X-ray diffraction is of low quality and the structure was refined with only isotropical thermal parameters. Although no reliable bond lengths and angles are given, the molecular structure of **13**, which is depicted in Figure 2.16, supports the spectroscopic results and the composition of this unusual compound. The rhenium atom reveals a pentagonal bipyramidal environment, in which the organic ligand is accommodated in the equatorial plane and the axial positions are occupied by a chloro and a methoxo ligand. Interestingly, the $\{dpic(i\text{-}Bu_2tu)_2\}^{2-}$ ligand does not coordinate via its oxygen atoms. It coordinates to the rhenium center as a pentadentate ligand using the N atom of the pyridyl ring, two N atoms and two S atoms of thiourea moieties. This is in the agreement with the high frequency of the absorption corresponding C=O stretches observed in IR spectrum.

2.5 Summary and Conclusions

N,N-Dialkylbenzoylthioureas are versatile ligands, which form stable complexes with rhenium and technetium. Irrespective of the oxidation states of the metals and/or the cores, they act as monoanionic chelates. The bonding situation inside the chelate rings manifests a high degree of delocalization of electron density, which also includes the exocyclic C–N bonds. The composition of the coordination sphere of the metal ions can be controlled by the reaction conditions applied and by co-ligands such as phosphines or alkoholates.

In solvents containing traces of water, the methoxo complex **3c** is hydrolyzed and then condensed under formation of the oxo-bridged dimer **4c**. By the addition of MeOH, a reversible conversion into **3c** was observed. Under the same conditions, the *m*-phthaloyl(bis-N,N-dialkylthiourea) complexes **11**, the solution of which contain a mixture of *syn* and *anti* isomers, are converted to a mixture of tetranuclear complexes **12** and hitherto uncharacterized oligomers and polymers $\mathbf{12^n}$.

An additional donor atom such as a pyridyl residue in the ligand sphere can change the coordination behavior of benzoylthioureas. The H_2picbtu is suitable to form the neutral O,S chelate **10,** while the H_2dpic(*i*-Butu)$_2$ ligand preferably coordinates to rhenium via the N and S atoms of thiourea moieties to form the pentagonal bipyramidal complex **13**.